Nonlinear nanopolaritonics: Finite-difference time-domain Maxwell–Schrödinger simulation of molecule-assisted plasmon transfer

Kenneth Lopata and Daniel Neuhauser[a)]
Department of Chemistry and Biochemistry, University of California, Los Angeles, Los Angeles, California 90095-1569, USA

The effect of nonlinear excitations of a nearby two-state dipolar molecule on plasmon transfer across a pair of spherical gold nanoparticles is studied numerically using a split field finite-difference time-domain Maxwell–Schrödinger approach [K. Lopata and D. Neuhauser, J. Chem. Phys. **130**, 104707 (2009)]. It is observed in the linear response regime that the molecule has a drastic effect on plasmon transfer; specifically, there is a Fano-type resonance that serves to scatter localized plasmons from *x*-polarization to *y*-polarization. With increasing nonlinearity of the molecular excitation, the scattering effect saturates due to the limited capacity of the molecule to absorb and radiate energy once the excited and ground states are equally populated. © *2009 American Institute of Physics*. [DOI: 10.1063/1.3167407]

I. INTRODUCTION

Near-field plasmon/molecule interactions have been the subject of intense theoretical,[1–8] and experimental[9–11] research due to their wide ranging application in nanoscale devices such as molecular sensors[12] and plasmonic circuits.[13]

The applications of plasmon/molecule systems are of two types. The first direction utilizes plasmon→molecule interaction, where strong fields near the surface of plasmon-carrying metal structures can be directed into nearby molecules and enhance their response. This type of interaction is exploited in surface enhanced Raman spectroscopy[10,14,15] or in plasmonically enhanced fluorescence.[16–19]

The second direction is the reverse, where the molecular response can influence plasmon resonances or even induce plasmons in nearby metal structures.[1,2,9,11] Molecule →plasmon interactions have shown theoretical utility as switching elements. Specifically, they have been shown to scatter localized surface plasmon polaritons (LSPPs) between plasmon polarizations[1,2] and gate plasmon transfer through fork junctions.[2] The study of molecule-mediated LSPP transfer is called nanopolaritonics.

Possible approaches to modeling these interactions include time-dependent density functional theory,[4,20] self-consistent Maxwell-optical Bloch equations,[5,8,21] many-body Green's functions coupled to mean-field Hartree–Fock,[7] multipole expansions,[6] extended Mie theory/multilevel density matrix approaches,[19] and nonlinear Maxwell–Schrödinger formalisms for two level molecules under laser light.[22,23]

The drawbacks to these methods are either large computational burden (and therefore a limited system size) or assumptions of simplified nanoparticle geometry. The ideal theoretical treatment of nanopolaritonic systems requires a multiscale approach, wherein the currents in an arbitrary shaped metal nanostructure and the fields around it are treated classically, while the molecule is treated rigorously using quantum mechanics. To this end, we previously reported a split field finite-difference time-domain (FDTD) approach which used linear response random phase approximation (RPA) for the molecule.[1] Here we extend on those results by not assuming linear response and instead the full density matrix for the two-level molecule is evolved in time, which captures nonlinear (e.g., multiharmonic) effects. Nonlinear effects are especially important when the molecule is under strong fields, as is the case in most nanoscale devices.

In this paper we demonstrate that nonlinear effects play a vital role in molecule→plasmon interactions. Specifically, the linear response approximation breaks down under strong fields, and the ability of the molecule to induce plasmons on adjacent metal structures saturates. On the other hand, under these conditions the molecule exhibits multiharmonic emission, which can be exploited to make nonlinear nanopolaritonic devices.

In Sec. II, we start with a condensed description of the split field FDTD approach and move on to a detailed description of the nonlinear time evolution of the molecule. Next, in Sec. III we present the results for a pair of spherical gold nanoparticles with a molecule midway between which demonstrate the breakdown of linear response. Section IV summarizes our results.

II. THEORY

The overall approach is similar to our previous work.[1] We evolve the fields and currents classically using FDTD[24,25] and evolve the currents on the two-level molecule quantum mechanically using a linear Hamiltonian and the full density matrix for the molecule.

a)Electronic mail: dxn@chem.ucla.edu.

131, 014701-1

A. FDTD formalism

To avoid the nonphysical self-interaction of the molecule with its own field we split the currents and electric and magnetic fields into two parts: one part due to the molecule (denoted with m subscript) and the other part (denoted with p subscript) due to everything else, which will subsequently act on the molecule,

$$E_{\text{tot}}(r,t) = E_p(r,t) + E_m(r,t), \tag{1}$$

$$H_{\text{tot}}(r,t) = H_p(r,t) + H_m(r,t), \tag{2}$$

$$J_{\text{tot}}(r,t) = J_p(r,t) + J_m(r,t). \tag{3}$$

For clarity we henceforth drop the explicit space and time dependence of these quantities.

The resulting time evolution equations for the nonmolecular part are (see Ref. 1 for discussion and derivation) the following:

$$\frac{\partial H_p}{\partial t} = -\frac{1}{\mu_0} \nabla \times E_p, \tag{4}$$

$$\frac{\partial E_p}{\partial t} = \frac{1}{\epsilon_{\text{eff}}} \nabla \times H_p + \left(\frac{1}{\epsilon_{\text{eff}}} - \frac{1}{\epsilon_0}\right) \nabla \times H_m - \frac{1}{\epsilon_{\text{eff}}} J_p, \tag{5}$$

$$\frac{\partial J_p}{\partial t} = \alpha(r)J_p + \beta(r)E_{\text{tot}}, \tag{6}$$

and for the molecular part are the following:

$$\frac{\partial H_m}{\partial t} = -\frac{1}{\mu_0} \nabla \times E_m, \tag{7}$$

$$\frac{\partial E_m}{\partial t} = \frac{1}{\epsilon_0}(\nabla \times H_m - J_m). \tag{8}$$

The evolution of the molecular current J_m is discussed below in Sec. II B. The electric and magnetic constants in atomic units (a.u.) are given by $\epsilon_0 = 1/(4\pi)$ and $\mu_0 = 4\pi/c^2$, where the vacuum speed of light is $c = 137.04$ a.u. The space-dependent (i.e., material-dependent) constants $\alpha(r)$, $\beta(r)$ and $\epsilon_{\text{eff}}(r)$ in Eqs. (4)–(6) are defined according to[1,26]

$$\alpha(r) = -\gamma_D(r), \tag{9}$$

$$\beta(r) = \epsilon_0[\omega_D(r)]^2, \tag{10}$$

$$\epsilon_{\text{eff}}(r) = \epsilon_0\epsilon_{r,\infty}(r), \tag{11}$$

where $\epsilon_{r,\infty}(r)$, $\gamma_D(r)$, and $\omega_D(r)$ are the Drude asymptotic relative permittivity, damping constant, and plasma frequency, which were taken from Ref. 27.

B. Molecular current

The current on the molecule J_m is evolved quantum mechanically in a density matrix formalism. The Von Neumann equation (in atomic unit) for the two-level molecule is

$$i\frac{\partial \rho(t)}{\partial t} = [H(t),\rho(t)] - i\gamma_m\rho(t), \tag{12}$$

where $\rho(t)$ is the density matrix for the molecule, $H(t)$ is the linear time-dependent molecular Hamiltonian, and γ_m is a matrix describing the phenomenological damping of molecular excitations. The damping matrix takes the form

$$\gamma_m = \begin{pmatrix} \gamma_1 & \gamma_2 \\ \gamma_2 & \gamma_1 \end{pmatrix}, \tag{13}$$

where the on-diagonal damping element γ_1 is the inverse of the T_1 dephasing time and γ_2 is the inverse of the T_2 dephasing time,

$$\gamma_1 = 1/T_1, \tag{14}$$

$$\gamma_2 = 1/T_2, \tag{15}$$

with $\gamma_1 < \gamma_2$. The values of T_1 and T_2 are chosen to match the phenomenological values. The Hamiltonian in the presence of the external field at the location of the molecule $E_p(r_m,t)$ is

$$H(t) = \begin{pmatrix} 0 & \xi_m(t) \\ \xi_m(t) & \omega_m \end{pmatrix}, \tag{16}$$

where the on-diagonals are expressed in terms of the excitation frequency $\omega_m \equiv \omega_2 - \omega_1$, and the off-diagonals arise from the coupling of the molecular dipole moment to the external field: $\xi_m(t) \equiv \mu_m \cdot E_p(r_m,t)$.

Analogous to what is done in the RPA, we introduce three quantities in terms of the matrix elements of the density matrix,

$$X \equiv \text{Re}[\rho_{21}], \tag{17}$$

$$Y \equiv \text{Im}[\rho_{21}], \tag{18}$$

$$Z \equiv \rho_{22}. \tag{19}$$

This converts the time evolution equation (12) into three coupled equations,

$$\frac{\partial X(t)}{\partial t} = \omega_m Y(t) - \gamma_2 X(t), \tag{20}$$

$$\frac{\partial Y(t)}{\partial t} = -\omega_m X(t) + 2\xi_m(t)Z(t) - \xi_m(t) - \gamma_2 Y(t), \tag{21}$$

$$\frac{\partial Z(t)}{\partial t} = -2\xi_m(t)Y(t) - \gamma_1 Z(t), \tag{22}$$

which are then evolved alongside the fields. Note that these equations are exact, i.e., they use the RPA notation but not the linear response approximation.

The current on the molecule is evaluated according to [see Eq. 29 in Ref. 1]

$$j_m(t) = -2\omega_m\mu_m Y(t), \tag{23}$$

which is then extrapolated onto the FDTD grid via a Delta function

Pair of spherical gold nanoparticles with molecule between
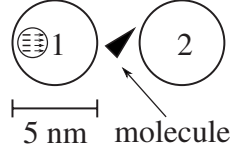
FIG. 1. The modeled system of two spherical gold nanoparticles with an xy-oriented molecule midway (molecule size not to scale). At $t=0$, the system is initialized with a Gaussian current at the left side of the left nanoparticle (shown as an inset circle).

$$J_m(\mathbf{r},t) = \mathbf{j}_m(t)\,\delta(\mathbf{r}-\mathbf{r}_m). \tag{24}$$

For simplicity, the Delta function in Eq. (24) is simply $0.25dV$ on the four nearest points on the Yee lattice,[24,25] where dV is the volume of each voxel. Note that these points must lie in the vacuum for this to be valid, and the whole formalism assumes that the molecule is sufficiently far from the metal surface such that electron tunneling can be neglected.

III. RESULTS

To investigate the effects of the molecule on LSPP transfer, we modeled two spherical $b=2.5$ nm radius gold nanoparticles separated by a center to center distance of $3b = 7.5$ nm, with an xy-oriented molecule placed midway between (see Fig. 1). The system studied here had a total volume of $44 \times 32 \times 32$ nm^3, grid spacings of $dx=dy=dz = 0.53$ nm, and a total number of grid points of $N = 327\,000$. The convergence of results with respect to the grid spacing was checked for values of 0.13, 0.27, 0.53, and 0.80 nm; 0.53 nm was chosen as a good tradeoff between accurate and computational efficiency. All simulations were run for 2500 a.u. time with a time step of 0.9 times the Courant stability limit,[25] which equals $dt=0.038$ a.u. $\approx 10^{-3}$ fs. At each time step an absorbing boundary condition (ABC) was applied to remove reflections from the edge of the grid. The form of ABC used was a space-dependent function $f(\mathbf{r})$ which in one dimension takes the form

$$f(x) = \begin{cases} 1, & x < x_{\max} - w \\ \exp\left[-\dfrac{(x-x_{\max}+w)^2}{(-w^2/\ln h)}\right], & x \geq x_{\max} - w. \end{cases} \tag{25}$$

The values of the Drude, simulation, and ABC parameters are shown in Table I.

At $t=0$, an x polarized spherical Gaussian current was initialized near the left side of the first nanoparticle according to

$$J_{x,1}(\mathbf{r},t=0) = \frac{J_0}{(2\pi)^{3/2}\sigma^3}\exp\left[-\frac{(\mathbf{r}-\mathbf{r}_g)^2}{2\sigma^2}\right], \tag{26}$$

where $\mathbf{r}_g$ is the center of the Gaussian, σ is the width, and J_0 is the norm. All other fields and currents were initialized as zero. This rather unphysical pulse was used to allow the LSPP pulse to propagate across the nanoparticle before acting on the molecule. A pulse was used rather than a more realistic plane-wave excitation so that subsequent Fourier

TABLE I. Summary of material and simulation parameters. All values with units are in atomic unit.

Gold	Molecule	Grid	Time	ABC
$\omega_D=0.33$	$\omega_m=0.10$			
$\gamma_D=0.028$	$\gamma_1=0.0001$	$N=327\,000$	$t_{\max}=2500$	$w=75$
$\epsilon_{r,\infty}=9.07$	$\gamma_2=0.001$	$dx=dy=dz=10$	$dt=0.038$	$h=0.2$
	$\mu_m=8$			

transform of the current signal would yield the full spectrum (at least in the linear regime). For reference, a complete list of simulation parameters is shown in Table I.

To quantify the transfer between the two nanoparticles, we measure the total currents on each as a function of time

$$J_{d,k}^{\text{tot}}(t) = \int_{\text{NP }k} J_d^{\text{tot}}(\mathbf{r},t)d^3\mathbf{r}, \tag{27}$$

where d refers to the three possible orthogonal polarizations $(d=x,y,z)$ and k refers to the nanoparticle index $(k=1,2)$. The time resolved currents yield the current spectra via the Fourier transform

$$J_{d,k}^{\text{tot}}(\omega) = \frac{1}{2\pi}\int_0^\infty J_{d,k}^{\text{tot}}(t)e^{-i\omega t}dt. \tag{28}$$

It is illuminating to discuss plasmon-molecule interactions over a variety of energy scales, ranging from the weak-excitation limit where linear response is valid to the high-excitation limit where nonlinear effects on the molecule become important. The best measure of the nonlinearity of the molecular response is the quantity $Z(t)$, which ranges between 0 and 1, with larger values corresponding to more nonlinear behavior, i.e., decreased ground state population. Physically, $Z(t)=0$ means the molecule is completely in its ground state before excitation, and $Z(t)=1$ corresponds to a fully populated excited state. For quantifying nonlinearity, we consider the root mean square (rms) value of $Z(t)$ over the first M time steps,

$$Z^{\text{rms}} \equiv \sqrt{\frac{1}{M}\sum_{i=1}^M [Z(t_i)]^2}. \tag{29}$$

Note that in the highly nonlinear regime, when the molecule rapidly oscillates between the states, Z^{rms} will level off at 0.5; therefore, numbers close to $Z^{\text{rms}}=0.5$ indicate saturation. The reason we chose the average value of $Z(t)$ is that the maximum value of it is often close to 1 and is therefore not a smooth function of the electric field strength and therefore the nonlinearity; E_p^{rms} was similarly used as a measure of the strength of the external field acting on the molecule according to

$$E_p^{\text{rms}} \equiv \sqrt{\frac{1}{M}\sum_{i=1}^M |E_p(\mathbf{r}_m,t_i)|^2}. \tag{30}$$

For concreteness, we chose to calculate these rms values over the first 500 a.u. (12 fs) of time, as this is the time scale over which all of the interesting dynamics take place.

Current spectra on second nanoparticle for various external fields
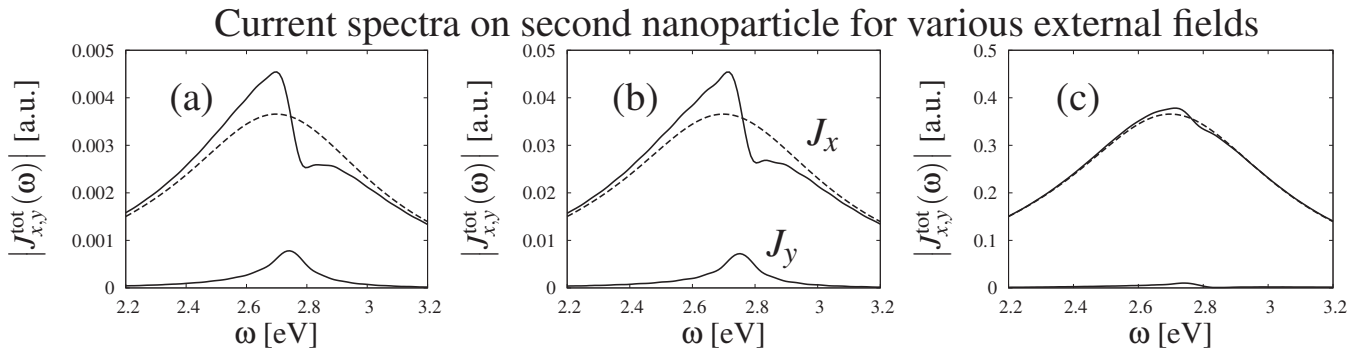
FIG. 2. The x-polarized (top curves) and y-polarized (bottom curve) current spectra on the second nanoparticle for three different initial current strengths without a molecule (dashed) and with a molecule (solid). The corresponding Z^{rms} and E_p^{rms} values for the three plots are (a) 0.0024, 6×10^{-5} a.u.; (b) 0.22, 6×10^{-4} a.u.; and (c) 0.39, 6×10^{-3} a.u. The molecule enhances the x current for frequencies below the molecular resonance and scatters energy to the y polarization for frequencies above. In the weak excitation limit, this Fano resonance scales linearly with the applied field, but it saturates for higher field strengths.

Figure 2 shows the x and y current spectra for the second nanoparticle for three different initial x-polarized currents, both with a molecule (solid lines) and without a molecule (dashed lines). For low excitation, the molecule enhances the x-current for frequencies below the molecular resonance and decreases it for frequencies above; there is also a strong induced y-current at the resonance frequency. The molecule absorbs radiation from the first nanoparticle and radiates xy-polarized light at a slightly different frequency. This radiation is then absorbed by the second nanoparticle. In other words, the xy-oriented molecule scatters energy to the y-polarization. This Fano-type resonance[28,29] is essentially identical to what was reported previously.[1,2] For stronger fields and corresponding large values of $Z(t)$ on the molecule, however, the resonance saturates and eventually disappears.

To elucidate this saturation effect, we measured the induced y current as a fraction of the x current on the second nanoparticle for a range of initial currents (and thus applied fields). To account for any grid artifacts, these quantities were measured for three values of dx (5, 10, and 15 a.u.) and extrapolated to $dx=0$. Figure 3 shows this fraction as a function of $E_p^{rms}(r_m)$, with all currents evaluated at the molecule's

resonance frequency ω_m. The rms of $Z(t)$ is shown (triangles; dashed line). In the weak excitation regime (low Z^{rms}), the percent energy transfer is roughly constant as the induced y currents scale lineally with the applied field. In the nonlinear regime (high Z^{rms}), however, the effect saturates and the percent induced y current decays to zero. Physically, the molecule has a limited capacity to absorb and radiate energy as its absorption is saturated once the excited state and ground state are equally populated ($Z=0.5$), which limits the magnitude of the currents induced by these fields on the nearby metal. Thus, the ability of a molecule to scatter LSPPs between polarizations is strongest in the linear response regime and quickly diminishes as the nonlinear effects become important. One caveat to these results is that under extremely strong fields, i.e., when $\xi_m = \mu_m \cdot E_p(r_m, t)$ is greater than the ionization energy, the molecule will ionize in which case the two-level approximation breaks down and alternate formalism is required.

IV. CONCLUSIONS

In summary, in the linear response regime a two-level molecule is predicted to have a significant impact on plasmon transfer through an array. Nonlinear effects on the molecule become significant for external fields (E_p) on the order of 0.005 a.u. ≈ 2.6 V/nm or greater, and in this nonlinear regime the ground and excited states become equally populated, which serve to limit the effect the molecule has on the surrounding metal. This phenomenon has several important implications. First, linear response treatments of molecules in plasmonic system may significantly overestimate the effect of the molecule on the plasmons, especially under strong fields. Caution must be taken when assuming linear response on the molecule, and any such treatments much carefully consider only the limit of weak fields acting on the molecule. Second, in real systems interesting phenomena centered around ω_m will eventually disappear as multiharmonic effects become more important. Finally, in principle the nonlinear excitation of the molecule can be used to build a nonlinear plasmonic device which exploits multiharmonic emission, such that a molecule with a low ω_m can couple to higher frequency plasmon modes. A molecule could, for ex-

Relative y-current on second nanoparticle compared to nonlinearity of molecular excitation

FIG. 3. The relative magnitude of the induced y-current on the second nanoparticle as compared to the x-current evaluated at the molecule's resonance frequency ω_m (circles; solid curve). As the nonlinearity of the molecular excitation increases, parameterized by the rms of $Z(t)$ (triangles; dashed curve), the relative magnitude of the y-current ratio decays to zero due to the finite capacity for the molecule to absorb and subsequently radiate energy.

ample, be used as a higher harmonic generator in a nonlinear plasmonic circuit, analogous to conventional frequency doubling birefringent crystals in macroscale nonlinear optics.[30] Although nonlinear molecular effects limit the potency of molecule→plasmon interactions, they do present intriguing opportunities for building nonlinear nanopolaritonic devices.

ACKNOWLEDGMENTS

[1] K. Lopata and D. Neuhauser, J. Chem. Phys. **130**, 104707 (2009).
[2] D. Neuhauser and K. Lopata, J. Chem. Phys. **127**, 154715 (2007).
[3] X. M. Hua, J. I. Gersten, and A. Nitzan, J. Chem. Phys. **83**, 3650 (1985).
[4] S. Corni and J. Tomasi, J. Chem. Phys. **117**, 7266 (2002).
[5] G. Colas des Francs, C. Girard, T. Laroche, G. Lévèque, and O. J. F. Martin, J. Chem. Phys. **127**, 034701 (2007).
[6] A. Govorov, G. Bryant, W. Zhang, T. Skeini, J. Lee, N. Kotov, J. Slocik, and R. Naik, Nano Lett. **6**, 984 (2006).
[7] D. J. Masiello and G. C. Schatz, Phys. Rev. A **78**, 042505 (2008).
[8] L. S. Froufe-Pérez and R. Carminati, Phys. Rev. B **78**, 125403 (2008).
[9] G. A. Wurtz, P. R. Evans, W. Hendren, R. Atkinson, W. Dickson, R. J. Pollard, A. V. Zayats, W. Harrison, and C. Bower, Nano Lett. **7**, 1297 (2007).
[10] J. A. Dieringer, K. L. Wustholz, D. J. Masiello, J. P. Camden, S. L. Kleinman, G. C. Schatz, and R. P. Van Duyne, J. Am. Chem. Soc. **131**, 849 (2009).
[11] J. Dintinger, S. Klein, F. Bustos, W. L. Barnes, and T. W. Ebbesen, Phys. Rev. B **71**, 035424 (2005).
[12] J. Homola, S. S. Yee, and G. Gauglitz, Sens. Actuators B **54**, 3 (1999).
[13] E. Ozbay, Science **311**, 189 (2006).
[14] K. Kneipp, Y. Wang, H. Kneipp, L. T. Perelman, I. Itzkan, R. R. Dasari, and M. S. Feld, Phys. Rev. Lett. **78**, 1667 (1997).
[15] S. Nie and S. R. Emory, Science **275**, 1102 (1997).
[16] F. Tam, G. P. Goodrich, B. R. Johnson, and N. J. Halas, Nano Lett. **7**, 496 (2007).
[17] K. T. Shimizu, W. K. Woo, B. R. Fisher, H. J. Eisler, and M. G. Bawendi, Phys. Rev. Lett. **89**, 117401 (2002).
[18] J. Lee, A. Govorov, J. Dulka, and N. Kotov, Nano Lett. **4**, 2323 (2004).
[19] P. Johansson, H. Xu, and M. Käll, Phys. Rev. B **72**, 035427 (2005).
[20] L. Zhao, J. Am. Chem. Soc. **128**, 2911 (2006).
[21] C. M. Bowden and J. P. Dowling, Phys. Rev. A **47**, 1247 (1993).
[22] A. K. Gupta and D. Neuhauser, Int. J. Quantum Chem. **81**, 260 (2001).
[23] E. Lorin, S. Chelkowski, and A. Bandrauk, Comput. Phys. Commun. **177**, 908 (2007).
[24] Kane Yee, IEEE Trans. Antennas Propag. **14**, 302 (1966).
[25] A. Taflove and S. Hagness, *Computational Electrodynamics: The Finite-Difference Time-Domain Method* (Artech House, Boston, 2005).
[26] S. K. Gray and T. Kupka, Phys. Rev. B **68**, 045415 (2003).
[27] A. Vial, A.-S. Grimault, D. Macías, D. Barchiesi, and M. L. de la Chapelle, Phys. Rev. B **71**, 085416 (2005).
[28] U. Fano, Phys. Rev. **124**, 1866 (1961).
[29] D. Neuhauser, T.-J. Park, and J. I. Zink, Phys. Rev. Lett. **85**, 5304 (2000).
[30] N. Bloembergen, *Nonlinear Optics*, 4th ed. (Addison-Wesley, Reading, 1996).